Demystifying mist explosion hazards

Stephanie El - Zahlanieh[1], Idalba Souza Dos Santos[1], Hugo Tostain[1], Alexis Vignes[2], Olivier Dufaud[1], Simon Gant[3]

[1] Reactions and Chemical Engineering Laboratory, University of Lorraine – CNRS, Nancy, France

[2] INERIS, Parc Technologique ALATA, BP 2, F-60550, Verneuil-en-Halatte, France

[3] Health and Safety Executive (HSE), Harpur Hill, Buxton, SK17 9JN, UK

It is essential that chemical and petrochemical industries take into account potential fire and explosion hazards as part of their risk assessments. Such hazards are sometimes related to flammable mists that can be generated by fluid releases from pressurized pipes or vessels, from condensation of hot vapours, or from splashing, etc. A recent study showed that around 10% of notified releases in the UK Offshore Hydrocarbon Release Database involved flammable mists. Analysis of the French and German ARIA and ZEMA databases also identified dozens of previous significant mist incidents. Despite this, there is limited guidance on hazardous area classification for flammable mists. Whilst classification of flammable gases and dusts is well established, there is a need for scientific evidence to support the classification of flammable mist hazards.

To address this knowledge gap, this paper presents an extensive study of diesel, biodiesel, and light fuel oil mists. These high-flashpoint liquid fuels were chosen as they have a high industrial interest and were involved in many reported incidents. A Venturi-based mist generation system was used to ensure the control of the fuel concentration, the fuel/air ratio and a well-defined droplet size distribution. Mists with mean droplet diameters ranging from 5 to 100 µm were thus obtained. Experiments were carried out in a modified apparatus based on the standardized 20 L explosion sphere where the experimental conditions, including the air injection pressure to the ignition delay time, were varied. In the first set of tests, the minimum ignition energy, lower explosive limit and explosion severity of the fuels were determined at 40°C and atmospheric pressure. In order to examine the impact of the fuel vapour/liquid ratio on the explosion behaviour, tests were undertaken with an increasing sphere temperature from 30°C to 80°C. Results showed that the surrounding temperature had a significant effect on the thermo-kinetic explosion parameters P_{ex} (explosion overpressure) and dP/dt_{ex} (rate of pressure rise). The value of dP/dt_{ex} increased markedly from approximately 24 bar.s^{-1} at T = 30°C to approximately 314 bar.s^{-1} at T = 80°C for a diesel mist concentration of 123 g.m^{-3}. These findings were compared to numerical data calculated using combustion software. The influence of the temperature on the evolution of the droplet size distribution and the evaporation rate of droplets was also studied. In addition, a specifically designed metallic reservoir was used to pressurize and preheat the fluid before injection to mimic industrial leaks that could trigger hazardous explosions. The influence of such parameters on the mist explosion risk assessment was then assessed.

The work presented in this paper improves our understanding of the physics behind mist explosions of high-flashpoint fuels. It also demonstrates the possibility of classifying hazardous mist areas using certain dimensionless numbers, such as the Ohnesorge and Reynolds numbers (which characterize droplet hydrodynamics) as well as the Spalding number (which characterizes droplet thermal behaviour).

Acknowledgement: The contribution by Simon Gant to this work was funded by the Health and Safety Executive (HSE). The contents, including any opinions and/or conclusions expressed, are those of the authors alone and do not necessarily reflect HSE policy.

Keywords: hydrocarbon aerosols, high-flashpoint fuels, mist hazards, explosions, flammability, risk assessment, process safety

Introduction

Over the years, the chemical and petrochemical industries have witnessed a significant number of explosions not only due to gases, vapours, or dusts, but also due to mists (Santon, 2009). The ATEX regulations[1] acknowledge the presence of the hazards due to flammable mists, but their classification is still limited to the flashpoint of the liquid in question. Several studies have shown that even high-flashpoint fluids, if aerosolised, can ignite and give rise to explosions (e.g. Eichhorn, 1955; Eckhoff, 2005).

Whilst classification of flammable gases and dusts is well established, the classification of aerosols is less clear. The aim of this paper is to counterbalance the lack of knowledge present in this field by providing scientific data to help support mist risk assessment and hence 'demystify mist explosion hazards'. This paper examines diesel, biodiesel, and light fuel oil mists. These high-flashpoint liquid fuels were chosen because they are widely used in industry and have been involved in numerous accidents. Experiments were conducted in a customized apparatus based on the conventional 20 L explosion sphere using a range of different air injection pressures and ignition delay times. After characterizing the mist cloud under atmospheric conditions, the minimum ignition energy (MIE), lower explosive limit (LEL), and explosion severity of each fuel were determined in the first set of experiments. The second set of experiments studied the impact of the fuel vapour/liquid ratio on the explosion severity of the fuels, which was examined across a range of different initial sphere and liquid temperatures. Finally, dimensionless numbers were mentioned along with a phenomenological study to better understand the physics of high-flashpoint fuel mist explosions.

[1] https://ec.europa.eu/growth/sectors/mechanical-engineering/atex_en (accessed 11.9.2021).

Literature Review

The ignitability and explosion severity of mists have long been a subject of interest, dating back to the early 1950s. Eichhorn (1955) first introduced the possibility of mists igniting at temperatures below their flashpoint in his publication "Careful! Mists can explode". Consequently, studies started to take place to investigate the various aspects of this subject. For instance, Freeston et al. (1956) studied mist ignition by hot surfaces, specifically in crankcase explosions. Burgoyne (1957, 1963) examined the flammability limits of tetralin mists (1,2,3,4-tetrahydronaphthalene; flashpoint: 77 °C, 350 K) and the influence of changing the drop size. Many similar investigations were first performed on tetralin, including Burgoyne and Cohen (1954) and Singh and Polymeropoulos (1988), as it was a pure hydrocarbon that was easy to study and examine. Interest in industrial fuels subsequently began to rise. A reliable model for spark ignition of aerosol/vapour systems was, for instance, developed by Ballal and Lefebvre (1978, 1981). The model was tested against heavy fuel oil, diesel oil, and gas oil. Over a wide range of equivalence ratios, all of these fuels were estimated to have a MIE of a few millijoules for mists with Sauter Mean Diameters (SMDs) of around 30 µm. Bowen and Shirvill (1994) noted that diesel fuel has a sufficiently high flashpoint (i.e. > 55°C) that when it is held at ambient temperature and pressure it does not give rise to a hazardous area, but a pressurized leak, such as one from a flanged joint, could atomize diesel into a flammable mist. Maragkos and Bowen (2002) subsequently showed that impinging releases of commercial diesel and a Shell gas oil could ignite at temperatures below their flashpoint.

More recent studies of diesel and fuel oil aerosol ignition and combustion include the studies by Shehata et al. (2014), Lei et al. (2014), Gant et al. (2016), and Imran et al. (2018). Biodiesel mists, although industrially interesting, have seldom been studied. This fuel was recommended by the HSE for testing in the current work due to the range of substance properties for different biodiesels. Ignition experiments on biodiesel have been undertaken at Cardiff University as part of HSE's ongoing MISTS2 joint industry project[2].

Incident Review

In his book "Explosion hazards in the Process Industry", Eckhoff (2005) published case histories of fuel mist incidents in industries. One reported incident was caused by diesel mists in 1974 on the ship 'Reina del Pacifico'. Evaporation of diesel oil in the hotter regions of the crank case, followed by circulation to and condensation in the colder parts, is thought to have generated fine mists, resulting in a powerful explosion that spread to three other engines and led to 28 fatalities. Another reported incident on an offshore platform was mentioned by Santon (2009) where a diesel mist fire took place after a gas turbine leaked during a fuel changeover, resulting in diesel mist which was subsequently ignited by a hot surface. More recently, Lees et al. (2019) demonstrated that according to statistics from the UK Hydrocarbon Release Database (HCRD), diesel sources accounted for 20% of all recorded occurrences. In fact, 11 of the 48 mist/spray flash fires documented between 2000 and 2005 involved diesel releases.

Methodology

Fuels of interest

Following a fluid classification system established by HSE which categorized certain fuels according to their flashpoints and their ease of atomization (Gant et al. 2016; Bettis et al., 2017), diesel, biodiesel (Valtris Champlor), and light fuel oil (CPE energies - Total Energies) were chosen to be examined in this study. All three fluids are fuels of very high industrial interest on which various processes depend. Since a significant number of the reported incidents involved diesel fuel, it is the main focus of this study. Experimental investigations were carried out on the three fuels, but in order not to overload this paper, the findings on diesel mist will be presented along with some others concerning light fuel oil and biodiesel.

The table below presents the physicochemical properties of the three fuels of interest. These properties will play an important role in understanding the different ignition and explosion behaviours that the fuels exhibit once/if ignited.

Table 1: Physicochemical properties of the three fuels of interest

	Diesel	Light Fuel Oil	Biodiesel B100
Flashpoint (°C)	> 55	> 55	> 300
Boiling point (°C)	150 - 380	150 - 380	> 350
Kinematic viscosity ($mm^2.s^{-1}$)	2 – 4.5 @ 40 °C	< 7 @ 40 °C	65 @ 20 °C
Density ($kg.m^{-3}$)	750 - 850	830 - 880	914 - 920
Surface tension ($kg.s^{-2}$)	0.0275	0.025	0.0312
Flammability limits (%)	0.5 - 8	0.5 - 5	-
Vapour Pressure (kPa)	0.4	< 1	< 0.009
HSE Release Class (Gant et al., 2016)	Release Class I	Release Class I	Release Class III/IV

[2] https://www.hse.gov.uk/aboutus/assets/docs/shared-research-flammable-mist.pdf (accessed 11.9.2021)

It should be noted that at high temperatures the physicochemical properties would change. For instance, biodiesel might belong to the HSE Release Class IV as its viscosity decreases with increasing temperature. Moreover, the properties of biodiesel may vary depending on its manufacturing process and the original substrate. Indeed, Bettis et al. (2017) stated that the behaviour of this fuel can lie between Release Class III and IV.

Mist generation and characterization

Because vessel ruptures or leaks have highly uneven forms and can occur in a variety of situations, predicting the behaviour of a mist cloud is challenging. To better anticipate such behaviour, experiments should be conducted in settings as close to those seen in industrial accidents as feasible. There are a variety of techniques for creating mists including condensation of a saturated vapour, liquid pressurization, electrospray and mechanical injection. A siphon gravity-fed spray generating device was employed in this study. This system consisted of a Venturi junction with two inlets: a pressurized air inlet linked to a compressed air bottle, and a liquid inlet connected to a room-temperature fuel reservoir (El-Zahlanieh et al., 2021). Along with a custom control system, this Venturi-based generation assured the control of the fuel concentration, the fuel/air ratio and the droplet size distribution.

When investigating the flammability of oil mists, it is crucial to first characterize the mist cloud. According to Gant et al. (2016), accurately characterizing a mist before ignition is critical since the droplet size distribution, concentration, and turbulence of mists can all have a significant impact on their safety characteristics. Bowen and Cameron (1999) also stated that droplet sizes, overall equivalence ratios, droplet equivalence ratios, and pre-ignition turbulence levels for fuel clouds must all be quantified. The authors also emphasized the significance of temporal resolution in the characterising the mist behaviour.

In the present work, to characterize the mist cloud, measurements of the droplet size distribution (DSD) and the level of turbulence were first carried out under ambient conditions. The DSD was assessed using an in-situ laser diffraction sensor (Helos/KR-Vario by Sympatec GmbH). As the explosion vessel utilized for this study was completely closed, a modified replica mentioned by Santandrea et al. (2020) allowed visual access and was used for the characterization studies. The DSD was measured directly through the borosilicate glass windows by the Helos laser sensor, which had three high-resolution measurement ranges (R1, R3, and R5) ranging from 0.5 µm to 875 µm. The R3 lens was primarily utilized in this investigation because it covered a wide range of droplet sizes, from 0.5/0.9 µm to 175 µm. Two distributions per millisecond were acquired by the sensor which provided many output options such as the SMD, the median diameter (d_{50}), and many other representative diameters along with the volume, surface, and number distributions. It should be noted that to have an approximate value of the DSD near the kernel spark created by the ignition source, the height of the sensor was set to a height matching the position of this source.

Mist generation was maintained at an air injection pressure of 3 bar and for an injection duration depending on the required concentration. Table 2 depicts the DSD of the diesel mists generated under the specified conditions and for a duration of 4 seconds. Distributions using this nozzle appeared to be monomodal with mean droplet sizes ranging between 7 and 12 µm, but it should be underlined that diesel mists with DSD up to 100 µm were also achievable.

Particle Image Velocimetry was subsequently used to assess the level of turbulence attained by the diesel mist created in the modified sphere under specific conditions. A Neodym-Yttrium-Aluminum-Garnet (Nd:YAG) laser was used to emit a continuous wave laser sheet with a wavelength of 532 nm. The droplets, which had been dispersed through the sphere, were illuminated, allowing their time evolution to be tracked. A high-speed video camera was utilized to record videos at 2000 frames per second to trace the flow of the droplets. From the recorded videos, PIVlab 2.45 was utilized to perform image pre-processing, PIV analysis using interpolation methods, calibration, post-processing, and data validation (Thielicke, 2021). The data collected allowed the calculation of the root-mean-square velocity v_{rms}, a measure considered as a representative characteristic of the level of turbulence. Velocity measurements appeared to be mildly influenced by the liquid type as v_{rms} values of 1.78 m/s and 1.34 m/s were obtained for diesel and biodiesel mists respectively at the end of the injection.

Table 2: DSD of diesel mists under atmospheric condition at P_{inj} = 3 bar

D_{10} (µm)	SMD (µm)	D_{50} (µm)	D_{90} (µm)
7.8	9.5	9.7	11.9

Ignition and explosion apparatus

Modifications were made to convert the conventional 20 L explosion sphere used for dust explosion tests to mist explosion testing (El-Zahlanieh et al., 2021). The mist generation system was placed at the bottom of the sphere, the dust container was removed, and two electronic valves were fitted to control inlet flow rates and the liquid/air ratio. Before injecting the fuel/air mixture, the sphere was partially vacuumed to a calculated pressure, guaranteeing that atmospheric pressure was achieved when the mist was fully injected. This pressure was estimated using a set injection times that could be adjusted depending on the required mist concentration inside the vessel. A water jacket controlled the temperature of the sphere, preventing the sphere from overheating after an explosion under atmospheric conditions. Chemical ignitors with an energy of 100 J were used to ignite the dispersed mixtures, and two piezoelectric pressure sensors were employed to track the pressure-time evolution. A new control and data acquisition system was developed by LRGP and used in this experimental study. Tests were carried out at different ignition delay times t_v (time between end of the injection and the actuation of the ignition source) to study the influence of turbulence on the explosion severity. Furthermore, the initial temperature of the sphere was increased using the

water jacket. Tests were performed at 30 °C, 40 °C, 60 °C, and 80 °C for both diesel and light fuel oil and were then compared to the same tests repeated with liquid preheating in a metallic reservoir to mimic industrial leaks.

Evaporating droplets

Godsave (1953) proposed the d^2-law, a simplified model of droplet evaporation, in which the square of the droplet diameter decreases linearly with time in a diffusion-controlled process (Equations 1 to 8). It is widely accepted to depict the evaporation of a spherically-symmetric droplet in a stable environment when droplet interaction is minimal, and the droplet temperature is constant and uniform. Knowing that this is not the case in practice, and due to PIV measurements, a wet-bulb temperature is approximated and then turbulence is taken into account via Reynolds and Schmidt numbers integrated into the fuel evaporation constant as proposed by Gökalp et al. (1992) (Equation 9).

Table 3: Equations of the d^2 law

(1)	(2)	(3)	(4)
$d^2 = d_0^2 - Kt$	$K = 8D\frac{\rho}{\rho_l}\ln(1+B_T)$	$B_T = (1+B_M)^{\frac{1}{Le_v}} - 1$	$Le_v = \frac{\lambda}{\rho C_p D}$
(5)	(6)	(7)	(8)
$B_M = \frac{Y_{vs} - Y_\infty}{1 - Y_{vs}}$	$Y_{vs} = \frac{x_{vs}M_v}{x_{vs}M_v + (1-x_{vs})M_{air}}$	$x_{vs} = \frac{P_{sat}(T_s)}{P}$	$P_{sat}(T_s) = Ae^{\left(\frac{B}{T_s} - C\right)}$
(9)	(10)	(11)	
$K_t = 8D\frac{\rho}{\rho_l}\ln(1+B_T)\left(1 + 0.0276Re^{\frac{1}{2}}Sc^{\frac{1}{3}}\right)$	$B_T = \frac{C_{p,v}(T_\infty - T_d) + \frac{Q}{s}Y_{Ox,\infty}}{L_v}$	$B_M = \frac{Y_{Fs} - \frac{Y_{Ox,\infty}}{s}}{1 - Y_{Fs}}$	

Comparable calculations can be carried out in both quiescent and turbulent environments using the combustion enthalpy Q, oxygen mass fraction $Y_{Ox,\infty}$, and mass stoichiometric coefficient s (Equations 9 to 11). Furthermore, it is important to remember that the sphere is a closed chamber. As a result, the saturation pressure at a particular temperature should be addressed while defining the characteristics of the mist cloud. One limitation for this model is that it only considers the behaviour of a single droplet and does not take into account the saturation effect generated by neighbouring droplets vaporizing in the closed sphere, resulting in a saturation limit. In order to represent the evaporation of fuel droplets in the 20 L sphere, both turbulence and saturation influences were taken into account in our model. Fluid characteristics were taken from material safety data sheets and handbooks. It should be noted that the sedimentation phenomenon and its effect on the time evolution of the fuel concentration was not considered here.

Results and Discussion

Influence of the ignition delay time and the level of turbulence

The ignition delay time t_v is defined as the time between the end of an injection and the actuation of the chemical ignitors. This factor is known to be related to the initial turbulence level and, consequently, has a significant effect on the explosion severity thermo-kinetic parameters. For this study, tests were performed at six different ignition delay times starting from instantaneous ignition after injection to a delay of 500 ms. A diesel mist concentration of 123 $g.m^{-3}$ ± 2 $g.m^{-3}$ was injected into the 20 L sphere which was heated to 40 °C. Figure 1 depicts the variation of the maximum explosion overpressure P_{ex} and the maximum rate of pressure rise dP/dt_{ex} as the ignition delay time was increased. It can be seen that both thermo-kinetic parameters tended to decrease as t_v increased until reaching a time where no explosion occurred (t_v = 400 ms). This behaviour can be explained by the sedimentation phenomenon, which resulted in droplets depositing on the walls of the sphere over time, decreasing the average mist concentration present in the ignition zone until it fell below the LEL. During this period when sedimentation took place, the turbulence level represented by v_{rms} decreased from 1.78 $m.s^{-1}$ to about 0.6 $m.s^{-1}$ at 400 ms. A similar trend has previously been observed in dust explosion experiments.

The dP/dt_{ex} showed a steadier decrease with ignition delay time than the P_{ex} curve in Figure 1. This is because P_{ex} is related to the chemical thermodynamics of the explosion reaction, whilst dP/dt_{ex} is purely related to the combustion kinetics, which are strongly influenced by the turbulence level.

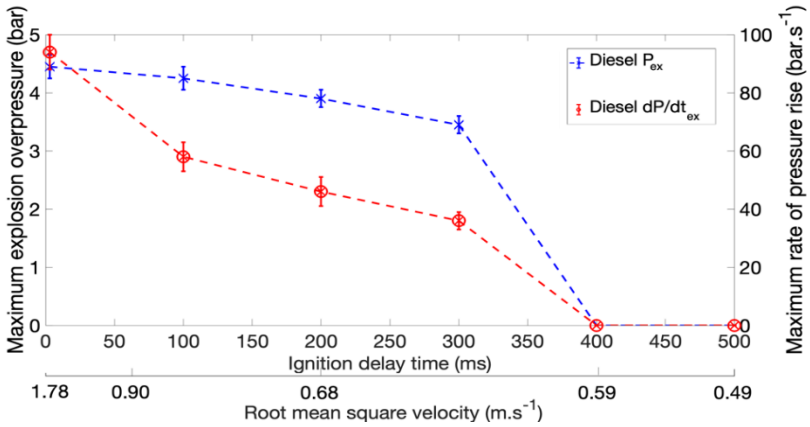

Figure 1: Influence of the ignition delay time t_v on both P_{ex} and dP/dt_{ex} at T = 40 °C and mist concentration of 123 g.m^{-3}

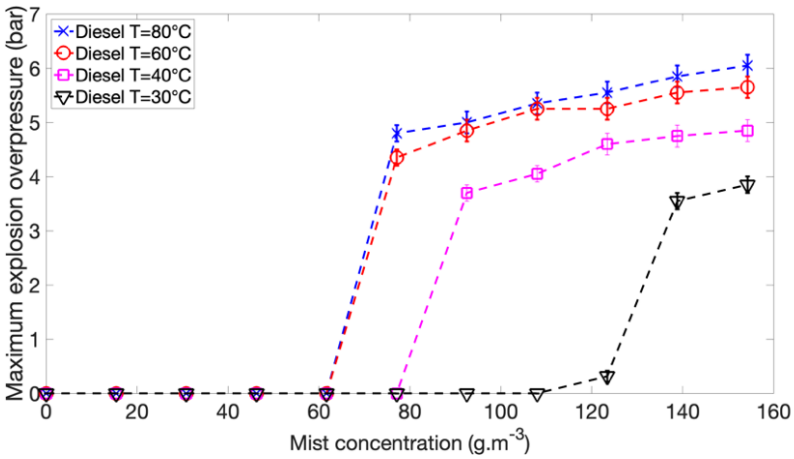

Figure 2: Influence of the initial sphere temperature and the diesel mist concentration on the explosion pressure P_{ex}

Influence of the sphere initial temperature

The possibility of oil leaks in a heated environment cannot be neglected. Indeed, mist releases can take place in hot crankcase engines, which can heat up to about 100 °C, and also in turbines, or heat transfer systems. For instance, in their literature review, Yuan et al. (2021) mentioned an explosion caused by a heat transfer fluid leak at a high temperature in LaGrange, USA. In order to assess such incidents, the 20 L sphere was heated to 40 °C, 60 °C, and 80 °C. Diesel and light fuel oil mists were tested at concentrations reaching about 155 g.m^{-3} with a SMD of 9.5 µm. Figures 2 and 3 illustrate the influence of this temperature increase on both P_{ex} and dP/dt_{ex}.

A first noticeable effect is that observed on the LEL. As the initial temperature was increased from 30 °C to 60 °C, the LEL decreased from approximately 123 g.m^{-3} to 77 g.m^{-3}. This decrease in the LEL can be explained by the increase of the fuel vapour phase surrounding the droplet, which facilitated ignition at higher temperatures. However, it can be seen that between 60 °C and 80 °C no change in the LEL was observed. In fact, once the initial temperature exceeded the flashpoint, very small changes were observed on the ignition sensitivity and on P_{ex}. Nevertheless, the influence on dP/dt_{ex} remained noticeable, showing that the kinetics of the mist combustion reaction, and especially the growth of the initial flame kernel, continue to be influenced by the initial surrounding temperature.

Figure 4 plots the vapour content of diesel mist clouds relative to the vapour content of a diesel mist cloud at the LEL at 30 °C (i.e., relative to the vapour content in a diesel mist produced in the 20 L sphere using an initial mass of 2.5 g, corresponding to 125 g.m^{-3}). For an initial droplet diameter of about 10 µm, the vapour / LEL ratio reaches unity at an initial temperature of about 330 K (about 57 °C) corresponding to the flashpoint of diesel fuel. However, at both 30 °C and 40 °C (303 K and 313 K), explosions took place with a P_{ex} of 0.3 bar and 4.6 bar and a dP/dt_{ex} of 24 bar.s^{-1} and 110 bar.s^{-1}, respectively, although the vapour ratio was lower than the LEL_{vapour}. Thus, it was clearly demonstrated that diesel can indeed ignite at a temperature below its flashpoint when dispersed as a mist. It should be kept in mind, however, that the initial mist temperature does not correspond to the local temperature at the ignition point/zone.

Similar tests were performed on light fuel oil for mist concentrations reaching about 162 g.m^{-3} with a DSD very similar to that of diesel. Table 4 summarizes the P_{ex} and dP/dt_{ex} values obtained during this series of experiments. Results were consistent with those obtained previously with diesel mists, in that both P_{ex} and dP/dt_{ex} increased gradually with mist concentration and initial temperature. Comparing the explosion severity of diesel and light fuel oil mists, diesel mists exhibited a slightly more severe behaviour as their P_{ex} and dP/dt_{ex} reached 6.0 bar and 535 bar.s^{-1} respectively, whereas for light fuel oil mists, 5.9 bar and 515 bar.s^{-1} respectively were observed. It can also be seen that an optimal mist concentration is rather difficult to pinpoint

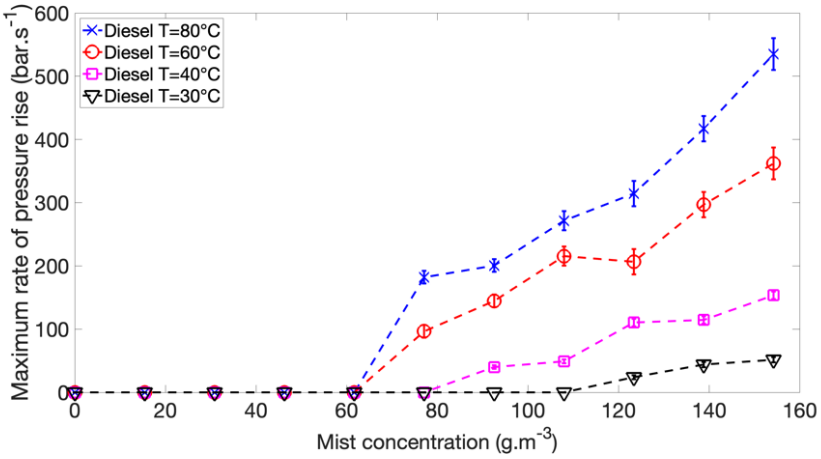

Figure 3: Influence of the initial sphere temperature and the diesel mist concentration on the explosion rate of pressure rise dP/dt_{ex}

in the case of mists, a situation different than that of gases which usually attain an optimal concentration close to that corresponding to stoichiometry. Indeed, Lemkowitz and Pasman (2014) stated that this optimum occurs in a fuel-rich mixture for dusts and mists, due to reduced conversion rates. Such behaviour can also be related to the concentration limitation due to saturation. Finally, it was observed that although already dangerous, mist explosions become more and more hazardous as the surrounding temperatures increase.

Biodiesel mist explosions were also tested; however, no explosions took place at the studied concentration range with 100 J ignitors. 5 kJ chemical ignitors were therefore used at T = 60 and 80 °C. The results from these tests are shown in Table 5.

Table 4: Influence of the initial sphere temperature and light fuel oil mist concentration on both thermo-kinetic explosion parameters

	P_{ex} (bar)			dP/dt_{ex} (bar.s^{-1})		
Mist concentration (g.m^{-3})	**T = 40 °C**	**T = 60 °C**	**T = 80 °C**	**T = 40 °C**	**T = 60 °C**	**T = 80 °C**
65	0	0	0	0	0	0
81	0	0	4.6	0	0	135
97	3.8	4.8	5.1	49	182	262
114	4.1	5.2	5.5	57	220	334
130	4.4	5.2	5.6	88	214	369
146	4.6	5.4	5.9	122	277	454
162	4.6	5.6	5.9	120.5	359	515

Table 5: Biodiesel mist explosion at T = 60 °C and 80 °C using an ignition energy of 5 kJ

	P_{ex} (bar)		dP/dt_{ex} (bar.s^{-1})	
Mist concentration (g.m^{-3})	**T = 60 °C**	**T = 80 °C**	**T = 60 °C**	**T = 80 °C**
80	0	0	0	0
91	0	4.6	0	135
103	4.9	5	182	263

The MIE tests were performed on diesel mists using a high-voltage spark ignition system that allowed the control of both the

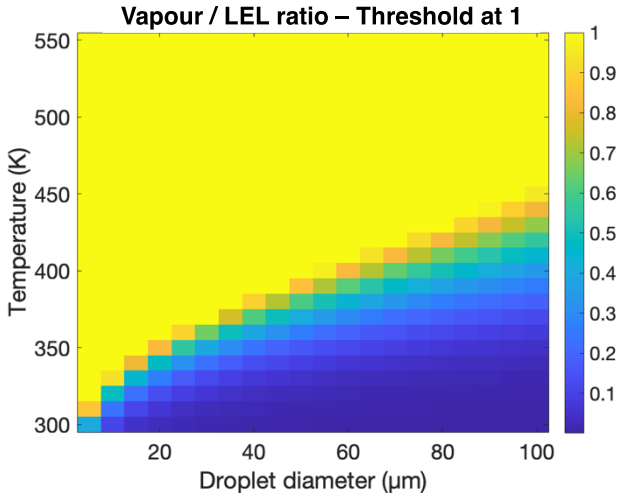

Figure 4: The vapour/LEL ratio (the threshold value is set at 1) as a function of the initial temperature and droplet size for a 2.5 g diesel mist cloud (125 g.m^{-3}) with a 3 ms delay time (similar to instantaneous ignition)

delivered current and the ignition time. The MIE of diesel mist with a concentration of 123 g.m^{-3} at a temperature of T = 40 °C was between 160 mJ and 316 mJ (with no ignition at 160 mJ). More tests are in progress to determine the influence of the mist concentration as well as the droplet size distribution on the MIE. Such experiments show that a single apparatus allows the determination of the lower explosive limit (LEL), the minimum ignition energy (MIE) and the explosion severity (P_{ex} and dP/dt_{ex}).

Influence of the sphere and liquid's initial temperature

In the first series of experiments, the liquid fuel was placed in a reservoir at ambient temperature before being injected into the sphere. Since compressed air was used to generate and breakup the liquid droplets, there were concerns that these conditions could affect the initial temperature before ignition as well as the explosion severity. Temperature measurements were therefore carried out using a thermocouple with an acquisition frequency of 20 Hz and a temperature measurement precision of ± 0.2 %. The thermocouple was placed at the centre of the sphere in the vicinity of the ignition source. The temperature was seen to decrease by a few degrees (not more than 5 °C) and then quickly increased to the initial set temperature. To assess the possible effect of this brief temperature drop, diesel fuel was heated in a metallic reservoir up to 40 °C and 80 °C prior to injection into the sphere, to match the temperature of the sphere. Figures 5 and 6 illustrate the influence of this preheating of the fuel on the explosion severity at T = 80 °C. It can be seen that, taking into account the error bars, preheating the diesel fuel did not have a significant effect on the explosion severity. The observed shifts may have been due to the change in fluid properties with the rise in temperature (e.g., the decrease of fuel viscosity).

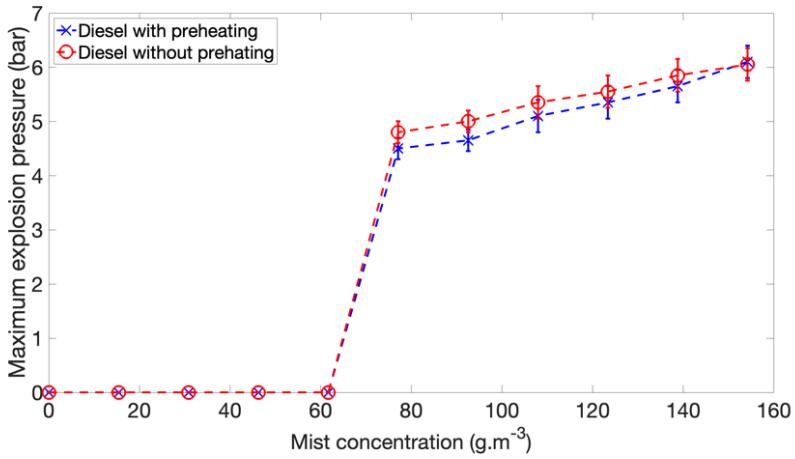

Figure 5: Influence of the diesel mist concentration on the explosion pressure P_{ex} with and without preheating the fuel before injection, T_{sphere} = 80°C

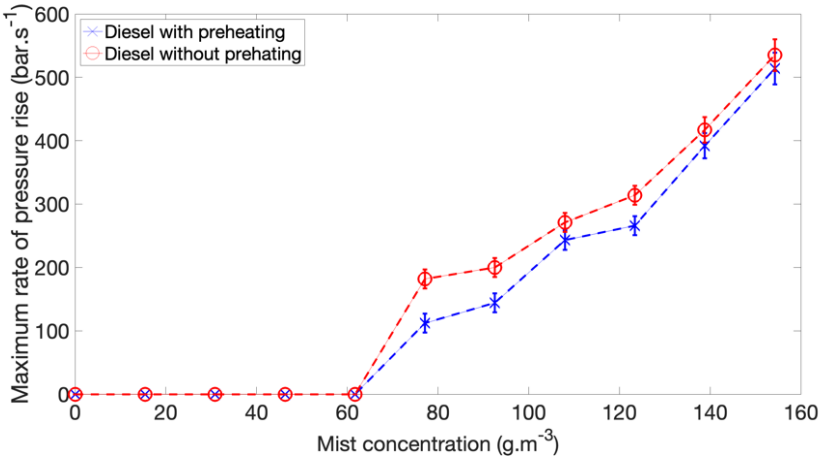

Figure 6: Influence of the diesel mist concentration on the explosion rate of pressure rise dP/dt_{ex} with and without preheating the fuel before injection, T_{sphere} = 80°C

Table 6 shows the results obtained at T = 40 °C which confirm the mild influence of liquid preheating. However, it can be seen that the LEL did change from 93 g.m^{-3} without preheating to 108 g.m^{-3} with preheated. This finding was rather hard to explain and could be linked to either experimental variability or the change in the liquid properties (and hence the DSD) arising from the change in temperature. Further characterization tests would be required in order to better understand this difference.

Table 6: Comparison of P_{ex} and dP/dt_{ex} of diesel explosions at T = 40 °C with and without fuel preheating

	P_{ex} (bar)		**dP/dt_{ex} (bar.s^{-1})**	
Mist concentration (g.m^{-3})	**with preheating**	**without preheating**	**with preheating**	**without preheating**
77	0	0	0	0
92	0	3.7	0	40
108	3.8	4.1	51	49
123	4.5	4.6	88	111
138	4.6	4.7	108	115
154	4.6	4.8	111	154

Dimensionless numbers and liquid classification

Droplet formation:

The nozzle used in this study was a twin fluid external mixing atomizer. Droplet formation was governed by several properties, notably those of both fluids (fuel and air) and their relative velocities. To estimate droplet formation under different conditions and to examine the influence of such conditions on the mean drop size, Inamura and Nagai (1985) and Elkotb (1982) proposed the following two empirical correlations, respectively (Table 7):

Table 7: Influence of Weber, Reynolds and Ohnesorge numbers on the Sauter mean diameter

(12)	(13)
$\frac{SMD}{t} = \left[1 + \frac{1680Oh^{0.5}}{We\left(\frac{\rho_L}{\rho_A}\right)}\right]\left[1 + \frac{0.065}{\left(\frac{\dot{m}_A}{\dot{m}_L}\right)^2}\right]$	$SMD = 51 d_0 Re^{-0.39} We^{-0.18} \left(\frac{\dot{m}_L}{\dot{m}_A}\right)^{0.29}$

where t is the initial film thickness $\left(t = \frac{D_0 h}{D_{an}}\right)$, D_0, the outer diameter of pressure nozzle, D_{an}, the diameter of the annular gas nozzle, and h, the slot width of the pressure nozzle.

It can be seen from both correlations that the SMD of the mist cloud is mainly governed by the droplet Reynolds number $Re = \frac{\rho_L d_0 U}{\mu_L}$, the droplet Weber number $We = \frac{\rho_L d_0 U^2}{\sigma}$, the Ohnesorge number $Oh = \frac{\mu_L}{\sqrt{\rho_L \sigma t}}$, and the ratio between the air and liquid mass flow rates. The temperature of both air and liquid should be considered, as their physical properties will change if heated: the fuel viscosity, density and surface tension will decrease when the temperature increases. Consequently, atomization will be enhanced and SMD will decrease (Shah and Ganesh, 2018), promoting droplet vaporization. The importance of the ease of atomization of the fluids in question is highlighted in the HSE liquid classification as the Ohnesorge number was used as a base dimensionless number to classify selected industrial fluids into four different release classes. This, therefore, demonstrates the prominence of taking liquid properties into account while examining their flammability and explosivity.

Droplet sedimentation and turbulence level:

Droplets floating in quiescent air fall at a speed determined by their shape and friction drag. Stokes' law governs the drag force F_d when the flow around a spherical droplet is laminar and there is no flow separation in the wake (Equations 14 to 16) (Table 8). Nevertheless, Stokes' law only applies to flows that are fully controlled by viscous forces, i.e., flows with low Reynolds numbers. The inertial forces become substantial at higher Reynolds numbers, and the drag force may rise due to the development of a wake and the potential separation of energy-consuming vortices. The presence of a boundary layer also causes another deviation from Stokes' rule (Lefebvre and McDonell, 2017). Many empirically derived functions are used to approximate experimental data collected by various investigators. In the case of this study, a rather turbulent flow exists before ignition that requires the application of another derived function. For a constant level of initial turbulence, an increase in the ignition delay time causes a reduction in the relative velocity between the droplets and their environment, leading to a lower drag force and hence more sedimentation. This sedimentation will therefore decrease the average mist concentration initially existing in the 20 L sphere and decrease the reactivity that enhances the explosion severity as shown in Figure 1.

Table 8: Stokes' law equations

(14)	(15)	(16)
$F_d = 3\pi d \mu_L U_R$	$C_D = \frac{F_d}{\frac{\pi}{4} d^2 \frac{\rho_A U_A^2}{2}}$	$C_D = \frac{24}{Re}$

In the experiments performed for this study, rather elevated temperatures were employed. Therefore, in addition to the turbulence level from the air injection at 3 bar, evaporation of the droplets may take place. Law (2006) proposed a correlation relating the drag coefficient C_D to the Spalding mass transfer number B_M for flows of Re < 200 (Equation 17).

$$C_D = \frac{23}{Sc^{0.14} Re}(1 + 0.276 Sc^{0.33} Re^{0.5})(1 + B_M)^{-1} \quad (17)$$

where $B_M = (Y_\infty - Y_s)/(Y_s - 1)$, the subscripts ∞ and s refer to far-field and surface values and Y is the vapour mass fraction. The correlation indicates that a rise in vapour mass fraction (due to elevated temperatures) leads to a reduction in the apparent drag coefficient. Indeed, numerical studies show that the droplet evaporation does not affect significantly the small-scale turbulent mixing but modifies the local buoyancy (Andrejczuk et al., 2006). In return, when the droplet sedimentation rate increases, the turbulent-kinetic energy increases. However, it should be kept in mind that, during its sedimentation and evaporation, the diameter of the droplets decreases, which reduces the settling velocity. At this stage, it is interesting to note that the preheating of the liquid (which favours atomization), will not have the same impact as the increase in the temperature of the sphere, which will tend to decrease C_D and therefore promote sedimentation (Figures 5 and 6).

Droplet ignition and combustion:

For a spark to cause ignition of a mist, the surrounding flammable mixture must first attain a sufficient ignition temperature. Convection and radiation play important roles. Once ignited, a flame may be viewed as a narrow reaction zone at the interface between the hot burnt gases and the fresh mixture of combustibles and oxygen. The combustion in the reaction zone provides the energy required to ignite the adjacent fresh mixture, allowing the flame to spread by conduction, radiation, radical propagation, or even a shockwave in the case of a detonation. There exist several dimensionless numbers that can govern these mechanisms, such as the Nusselt number Nu (Equation 18), which is the ratio of the convective and conductive heat transfer, the Stanton number (Equation 19), which is the ratio of the heat transferred into the droplets to the fluid heat capacity in forced convection flows, the Spalding heat transfer number B_T (Equation 20), which is the ratio of the available energy to the required energy for evaporation, the Lewis number Le (Equation 4), which is the ratio of the thermal diffusivity to the mass diffusivity.

(18)	(19)	(20)
$Nu = \frac{hd}{\lambda}$	$Sta = \frac{h}{\rho_{air} U C_p}$	$B_T = \frac{C_{p,v}(T_\infty - T_d)}{L_v}$

As the initial temperature increases, the energy required to vaporize the liquid droplets decreases, leading to an increase in the Spalding heat transfer number, hence an increase in the vapour mass fraction. This increase is translated into an easier ignition and a higher fuel vapour concentration in the sphere, which explains the decrease of the LEL with increasing temperatures. The increasing vapour-liquid ratio therefore facilitates the propagation of a flame into the mist.

For a given initial vapour-liquid ratio, a certain temperature should be attained for the mixture to ignite. As the liquid droplets are heated, they reach a limit where the heat losses are lower than the heat accumulated (the ratio represented by Sta). This leads to a self-heating phenomenon, leading to an increase in temperature until reaching the ignition of the flame kernel. Above a certain temperature, the initial vapour/liquid ratio does not have a significant effect on the propagation of the flame (provided it is high enough that vapour concentrations exceed the LEL). The physical processes governing the propagation of the flame are dominated by radiative and convective heat transfer, which can be expressed in terms of droplet Nusselt numbers. The level of turbulence also plays a role here as its increase leads to a higher convection coefficient and hence to an improved heat transfer towards the droplet. Combined with considerations on flame stretching, this can explain the decrease in the rate of explosion pressure rise as the turbulence level decreased as shown in Figure 1.

Once the ignition of the flame kernel takes place, the flame propagation leads to droplets' vaporization upstream of the flame front. Going back to Figure 4, the flame would already have been in the yellow zone where the vapour ratio exceeds the LEL as all liquid droplets ahead of the flame would be evaporated in the preheating zone, provided that the droplet size is sufficiently small.

Finally, it should be reminded that the flame propagation induces the expansion of the burnt gases and the generation of pressure waves ahead of the flame. Then, these waves collide with the unburnt mist, modifying its droplet size distribution and potentially ejecting droplets against the sphere's inner wall, hence reducing the local fuel concentration.

Conclusion and perspectives

The objective of this experimental study was to address the lack of knowledge present in the field of mist hazards by providing new scientific data to support mist risk assessment. Tests were undertaken on diesel, biodiesel, and light fuel oil mists: three high-flashpoint liquid fuels that are widely used in transport and heating industries which have been involved in numerous accidents. Experiments were conducted using a modified 20 L explosion sphere. The measurements showed that the explosion severity decreased as the ignition delay time was increased, due to the diminution in the turbulence level and the effect of droplet sedimentation. The fuels were tested at a range of different initial temperatures. As the initial temperature was increased from 30 °C to 60 °C, the vapour ratio was increased until reaching saturation and the LEL decreased from approximately 123 $g.m^{-3}$ to 77 $g.m^{-3}$. The explosion severity was also seen to increase with increasing initial temperatures. In addition to controlling the initial temperature of the 20 L sphere, tests were undertaken in which the fuels were preheated in a metallic reservoir to mimic industrial leaks. Finally, the use of various dimensionless heat transfer numbers was discussed as a means of analysing the flammability of fuel mists. The experimental study proved that high-flashpoint fuels can sustain explosions at temperatures below their flashpoint. The results reiterate the importance and necessity of having clearer and well-established guidelines and regulations on the risk assessment of flammable mists.

Glossary

Symbol	Definition		
B_T, B_M	Thermal and mass transfer Spalding numbers	C_D	Drag coefficient
C_p	Vapour phase heat capacity	d	Droplet diameter
D	Diffusivity coefficient	D_x	Diameter where x percent of the distribution has a smaller droplet size
K	Fuel evaporation constant	Le	Lewis number

L_v	Enthalpy of vaporization	M	Molar mass
$\dot{m}$	Mass flow rate	Oh	Ohnesorge number
P_{sat}	Saturation vapour pressure	Q	Heat of combustion
Re	Reynolds number	Sc	Schmidt number
t	Time	T	Temperature
t_v	Ignition delay time	U	Velocity
We	Weber number	x_{vs}	Vapour fraction
Y_{vs}	Vapour fraction at stoichiometry	λ	Thermal conductivity
ρ	Density	σ	Surface tension
μ	Dynamic viscosity	F or L	Fuel or Liquid
A	Air	v	Vapour phase
Ox	Oxygen	0	At t = 0
s	Stoichiometry		

References

Andrejczuk, M., Grabowski, W.W., Malinowski, S.P., Smolarkiewicz, P.K., 2006.Numerical simulation of cloud-clear air interfacial mixing: Effects on cloud microphysics. Journal of the Atmospheric Sciences, 63 (12), 3204-3225. https://doi.org/10.1175/JAS3813.1

Ballal, D.R., Lefebvre, A.H., 1981. A general model of spark ignition for gaseous and liquid fuel-air mixtures. Symposium (International) on Combustion, Eighteenth Symposium (International) on Combustion 18, 1737–1746. https://doi.org/10.1016/S0082-0784(81)80178-6 (accessed 11.9.2021)

Ballal, D.R., Lefebvre, A.H., 1978. Ignition and flame quenching of quiescent fuel mists. Proceedings of the Royal Society of London. A. Mathematical and Physical Sciences 364, 277–294. https://doi.org/10.1098/rspa.1978.0201(accessed 11.9.2021)

Bettis, R., Burrell, G., Gant, S., Coldrick, S., 2017. Area classification for oil mists - final report of a Joint Industry Project. RR1107 HSL report, UK. http://www.hse.gov.uk/research/rrhtm/rr1107.htm (accessed 11.9.2021)

Bowen, P.J., Cameron, L.R.J., 1999. Hydrocarbon Aerosol Explosion Hazards: A Review. Process Safety and Environmental Protection 77, 22–30. https://doi.org/10.1205/095758299529749 (accessed 11.9.2021)

Bowen, P.J., Shirvill, L.C., 1994. Combustion hazards posed by the pressurized atomization of high-flashpoint liquids. Journal of Loss Prevention in the Process Industries 7, 233–241. https://doi.org/10.1016/0950-4230(94)80071-5 (accessed 11.9.2021)

Burgoyne, J.H., 1963. The flammability of mists and sprays. Proc. 2nd Symp. on Chemical Process Hazards 1–5.

Burgoyne, J.H., 1957. Mist and spray explosions. Chemical Engineering Progress 53, 121–124.

Burgoyne, J.H., Cohen, L., 1954. The Effect of Drop Size on Flame Propagation in Liquid Aerosols. Proceedings of the Royal Society of London. Series A, Mathematical and Physical Sciences 225, 375–392.

Eckhoff, R.K., 2005. Chapter 3 - Explosions in Clouds of Liquid Droplets in Air (Spray/Mist), in: Eckhoff, R.K. (Ed.), Explosion Hazards in the Process Industries. Gulf Publishing Company, pp. 149–173.

Eichhorn, J., 1955. Careful! Mists can explode. Petroleum Refiner 34(11), 194–196.

Elkotb, M.M., 1982. Fuel atomization for spray modelling. Progress in Energy and Combustion Science 8, 61–91. https://doi.org/10.1016/0360-1285(82)90009-0 (accessed 11.9.2021).

El-Zahlanieh, S., Sivabalan, S., Tribouilloy, B., Benoit, T., Brunello, D., Vignes, A., Dufaud, O., 2021. Lifting the Fog Off Hydrocarbon Mist Explosions. Presented at the AIChE Spring Meeting 2021 & 17. Global Congress on Process Safety (GCPS).

Freeston, H.G., Roberts, J.D., Thomas, A., 1956. Crankcase Explosions: An Investigation into Some Factors Governing the Selection of Protective Devices. Proceedings of the Institution of Mechanical Engineers 170, 811–824. https://doi.org/10.1243/PIME_PROC_1956_170_072_02 (accessed 11.9.2021).

Gant, S., Bettis, R., Coldrick, S., Burrell, G., Santon, R., Fullam, B., Hill, H., Mouzakitis, K., Giles, A., Bowen, P., 2016. Area classification of flammable mists: summary of joint-industry project findings, IChemE Hazards 26 Conference, Edinburgh, UK, 24-26 May 2016. https://www.icheme.org/media/11775/hazards-26-paper-38-area-classification-of-flammable-mists-summary-of-joint-industry-project-findings.pdf (accessed 11.9.2021).

Godsave, G.A.E., 1953. Studies of the combustion of drops in a fuel spray—the burning of single drops of fuel. Symposium (International) on Combustion 4, 818–830. https://doi.org/10.1016/S0082-0784(53)80107-4 (accessed 11.9.2021).

Gökalp, I., Chauveau, C., Simon, O., Chesneau, X., 1992. Mass transfer from liquid fuel droplets in turbulent flow. Combustion and Flame 89, 286–298. https://doi.org/10.1016/0010-2180(92)90016-I (accessed 11.9.2021).

Imran, F., Morley, G., Anionwu., V., Saeed, M., Andrews, G., Phylaktou, H., 2018. Mist Explosions using the Hartmann Dust Explosion Equipment. In: XII ISHPMIE. 12th International Symposium on Hazards, Prevention and Mitigation of Industrial Explosions – XII ISHPMIE, 12-17 Aug 2018, Kansas City, MO, USA.

Inamura, T., Nagai, N., 1985. The relative performance of externally and internally-mixed twin-fluid atomizers, in: Proceedings of the 3rd International Conference on Liquid Atomization and Sprays. London, p. IIC/2/1-11.

Law, C.K., 2006. Combustion Physics. Cambridge University Press, Cambridge.

Lees, P., Gant, S., Bettis, R., Vignes, A., Lacome, J.-M., Dufaud, O., 2019. Review of recent incidents involving flammable mists. IChemE Hazards 29 Conference, Birmingham, UK. https://www.icheme.org/media/12613/hazards-29-paper-31-review-of-recent-incidents-involving-flammable-mists.pdf (accessed 11.9.2021).

Lefebvre, A.H., McDonell, V.G., 2017. Atomization and sprays, Second edition. ed. CRC Press, Taylor & Francis Group, CRC Press is an imprint of the Taylor & Francis Group, an informa business, Boca Raton.

Lei, Z., Lu, C., An, G.J., Xiong, C., Xie, L.F., 2014. Experimental Study on Combustion and Explosion Characteristics of Diesel. https://doi.org/10.4028/WWW.SCIENTIFIC.NET/AMR.1046.30 (accessed 11.9.2021)

Lemkowitz, S.M., Pasman, H.J., 2014. A Review of the Fire and Explosion Hazards of Particulates. KONA 31, 53–81. https://doi.org/10.14356/kona.2014010 (accessed 11.9.2021).

Maragkos, A., Bowen, P.J., 2002. Combustion hazards due to impingement of pressurized releases of high-flashpoint liquid fuels. Proceedings of the Combustion Institute, Proceedings of the Combustion Institute 29, 305–311. https://doi.org/10.1016/S1540-7489(02)80041-4

Santandrea, A., Gavard, M., Pacault, S., Vignes, A., Perrin, L., Dufaud, O., 2020. 'Knock on nanocellulose': Approaching the laminar burning velocity of powder-air flames. Process Safety and Environmental Protection 134, 247–259. https://doi.org/10.1016/j.psep.2019.12.018 (accessed 11.9.2021).

Santon, R.C., 2009. Mist fires and explosions – an incident survey. Proc. IChemE Hazards XXI Symposium & Workshop, Manchester, UK. https://www.icheme.org/media/9551/xxi-paper-054.pdf (accessed 11.9.2021).

Shah, P.R., Ganesh, A., 2018. Study the influence of pre-heating on atomization of straight vegetable oil through Ohnesorge number and Sauter mean diameter. Journal of the Energy Institute, 91 (6), pp. 828-834. https://doi.org/10.1016/j.joei.2017.10.006 (accessed 11.9.2021).

Shehata, M.S., ElKotb, M.M., Salem, H., 2014. Combustion Characteristics for Turbulent Prevaporized Premixed Flame Using Commercial Light Diesel and Kerosene Fuels. Journal of Combustion 2014. https://doi.org/10.1155/2014/363465 (accessed 11.9.2021).

Singh, A.K., Polymeropoulos, C.E., 1988. Spark ignition of aerosols. Symposium (International) on Combustion, Twenty-First Symposuim (International on Combustion) 21, 513–519. https://doi.org/10.1016/S0082-0784(88)80280-7 (accessed 11.9.2021).

Thielicke, W., 2021. PIVlab - particle image velocimetry (PIV) tool with GUI https://github.com/Shrediquette/PIVlab/releases/tag/2.53 (accessed 7.1.21).

Yuan, S., Ji, C., Han, H., Sun, Y., Mashuga, C.V., 2021. A review of aerosol flammability and explosion related incidents, standards, studies, and risk analysis. Process Safety and Environmental Protection 146, 499–514. https://doi.org/10.1016/j.psep.2020.11.032 (accessed 11.9.2021).